Journal of
Chemical Engineering & Process Technology

Sheriff and Nounou, J Chem Eng Process Technol 2017, 8:2
DOI: 10.4172/2157-7048.1000328

Research Article
Open Access

Improved Fault Detection and Process Safety Using Multiscale Shewhart Charts

M Ziyan Sheriff[1,2] and Mohamed N Nounou[1]*

[1]*Chemical Engineering Program, Texas A&M University at Qatar, Doha, Qatar*
[2]*Artie McFerrin Department of Chemical Engineering, Texas A&M University, College Station, TX 77843, USA*

Abstract

Process safety is a critical component in various process industries. Statistical process monitoring techniques were initially developed to maximize efficiency and productivity, but over the past few decades with catastrophic industrial disasters, process safety has become a top priority. Sensors play a crucial role in recording process measurements, and according to the number of monitored variables, process monitoring techniques can be classified into univariate or multivariate techniques. Most univariate process monitoring techniques rely on three fundamental assumptions: that process residuals contain a moderate level of noise, are independent, and are normally distributed. Practically, however, due to a variety of reasons such as modeling errors and malfunctioning sensors, these assumptions are violated, which can lead to catastrophic incidents. Fortunately, multiscale wavelet-based representation of data inherently possesses characteristics that are able to deal with these violations of assumptions. Therefore, in this work, multiscale representation is utilized to enhance the performance of the Shewhart chart (which is a well-known univariate fault detection method) to help improve its performance. The performance of the developed multiscale Shewhart chart was assessed and compared to the conventional chart through two examples, one using synthetic data, and the other using simulated distillation column data. The results of both examples clearly show that the developed multiscale Shewhart chart provides lower missed detection and false alarm rates, as well as lower ARL_1 values (i.e., quicker detection) for most cases where the fundamental assumptions of the Shewhart chart are violated. Additionally, the relative simplicity of the proposed algorithm encourages its implementation in practice to help improve process safety.

Keywords: Process monitoring; Fault detection and diagnosis; Shewhart chart; Multiscale representation; Wavelets

Introduction

Statistical process monitoring (SPM) plays a critical role in most process industries. Primary functions of SPM are to ensure that plants run safely within minimal down-time for maintenance, and to ensure that the end product is of a desired quality. SPM is generally carried out in two phases: fault detection, during which the faults in a particular process system are first identified, and fault diagnosis, during which the root cause of the fault is isolated and determined, after which action is taken to bring the process back to normal operating conditions [1]. Sensors play a crucial role as they need to ensure that the process operates as designed, and this is accomplished by monitoring different process variables to ensure the process are running smoothly. Quick, efficient, and accurate fault detection is required because it can help prevent major safety incidents from occurring, thus ensuring safety of life, property and economy. This paper currently only looks to examine and improve the fault detection aspect of process monitoring.

There are a number of methodologies that can be used to classify fault detection methods. Fault detection methods can be classified according to their dependency on models used. These can be quantitative model-based methods, such as observers or parity space [2], qualitative model-based methods, such as fault trees, digraphs, or even process engineering experts [3-6], or process-history (data-based) methods, such as Principal Component Analysis (PCA) and neural networks [7,8]. Accurate qualitative and quantitative model-based methods may not always be available, especially for complex processes with multiple process variables, and therefore data-based methods are often employed. Data-based methods rely on collecting fault-free data (under normal operating conditions), that are then used to design fault detectors, i.e., define the control limits. These limits are then applied on new process measurements (testing data), to detect potential faults (deviations or abnormalities) in processes. Data-based monitoring methods have been applied to detect anomalies in a wide variety of applications, from medical sensors [9], to wind turbines [10], to the petroleum industry [11]. Deviations in process variables can be due to a number of reasons, from faulty sensors to malfunctioning alarms, and therefore it is essential to address these concerns in order to prevent catastrophic incidents.

Anomalies in processes can lead to catastrophic incidents. One example of a catastrophic incident is the Texas City refinery explosion, at the British Petroleum's (BP) plant in Texas City, Texas, where an explosion killed 15 people and caused nearly 180 injuries. Although there were a number of factors that led to the incident, one of the main contributing factors was the fact that multiple level indicators and alarms in the raffinate tower malfunctioned, and provided incorrect readings [12]. This led the tower to over-pressurize and eventually explode once it came into contact with an ignition source [13]. Data-based techniques are an efficient way of observing a process to monitor deviations in multiple key process measurements, and this paper aims to improve the fault detection capability of a very simple monitoring chart, the Shewhart chart,in order to widen its applicability in practice, and hopefully prevent major industrial disasters such as the incident mentioned.

***Corresponding author:** Mohamed N Nounou, Department of Chemical Engineering, Texas A&M University at Qatar, Doha, Qatar, Tel: +97444230208; E-mail: Mohamed.nounou@qatar.tamu.edu

Received March 13, 2017; **Accepted** March 17, 2017; **Published** March 23, 2017

Citation: Sheriff MZ, Nounou MN (2017) Improved Fault Detection and Process Safety Using Multiscale Shewhart Charts. J Chem Eng Process Technol 8: 328. doi: 10.4172/2157-7048.1000328

Data-based techniques can be used to study trends of single process variables (univariate), or to analyze trends across multiple variables (multivariate). The Shewhart chart was one of the earliest (univariate) charts used for process monitoring purposes [14]. The chart is applied on process residuals, without the utilization of any filters. It is computationally simple to implement [15]. Other univariate charts, such as EWMA (Exponentially Weighted Moving Average) and CUSUM (Cumulative Sum) charts utilize the application of linear filters, before carrying out fault detection and can be more computationally expensive [16-18]. These charts may also require one or more tuning parameters to be modified, thus making the design of these charts increasingly computationally expensive and tedious. Process noise is often a concern in most process industries and can adversely affect the accuracy of fault detection techniques [4,19,20]. Charts with process memory such as CUSUM and EWMA may be able to address concerns related to process noise as they utilize filters. However, these filters are linear and may not be very effective at removing different types of noise or errors as they define a frequency threshold and anything above this threshold may be considered noise. The presence of process noise is not the only concern of these control charts. They also assume that process residuals being analyzed are independent (uncorrelated), and follow a normal (Gaussian) distribution [21]. However, in practice, real measurements might not necessarily satisfy these assumptions. In the past, many authors have looked into improving the fault detection abilities of particular techniques when process data violate one of these assumptions [22,23]. However, in practice, it may be possible that actual process data violate one or more of these assumptions. Therefore, more effective fault detection techniques that are able to simultaneously deal with process data that violate multiple assumptions are required. In addition, it is desirable that the developed technique is computationally simple, and relatively easy to implement in order to broaden its applicability.

One way to deal with these limitations of the conventional univariate fault detection methods is using wavelet-based multiscale representation. Multiscale representation has been shown to effectively deal with real process data as it allows efficient separation of important features from stochastic noise and provides wavelet coefficients that are approximately decorrelated and more Gaussian at multiple scales. Thus, it can help address most of the assumptions of the conventional univariate fault detection or control charts [24,25]. These advantages of multiscale representation will be utilized in this work to develop a multiscale Shewhart chart algorithm that will provide improved performance. Even though the ideas presented in this paper can be directly extended to other univariate control charts, this work focuses on the Shewhart chart due to its popularity and its computational simplicity [26]. These advantages of multiscale representation have been exploited by [27] who developed wavelet-based multiscale CUSUM and EWMA charts with improved fault detection abilities using autocorrelated process data. These techniques have been shown to improve the out-of-control average run length (ARL_1), which measures how long a particular technique takes to identify the presence of a fault. This is particularly important in terms of safety in process industries because faster detection allows more time to take corrective measures to bring a process back to its normal operating conditions. Other important metrics that can be used to assess the effectiveness of various fault detection techniques include the missed detection rate or the false alarm rate, which for certain applications can be as critical as the ARL_1.

Therefore, a proper evaluation of any fault detection technique requires assessing its performance with respect to all of these metrics. Unfortunately, the effect of multiscale representation on the performance of univariate control charts (especially under violation of their basic assumptions) and using all evaluation metrics (i.e., missed detection rate, false alarm rate, and ARL_1) has not been thoroughly studied. Therefore, the main objective of this work (which focuses on the Shewhart chart as an example of a univariate fault detection method) is to develop a multiscale form of the Shewhart chart that is easy to implement, and then assess its performance in comparison to its conventional counterpart under the violation of its three fundamental assumptions using various evaluation metrics. Such analysis should pave the road for similar ones using different univariate as well as multivariate fault detection methods.

This paper is structured as follows. First, an introduction to conventional univariate process monitoring is provided, along with a brief description of the Shewhart chart. Then multiscale wavelet-based data representation is explained, along with its advantages in process monitoring followed by a description of the developed multiscale Shewhart chart algorithm. The performance of the developed multiscale Shewhart chart is then analyzed through two illustrative examples, using simulated synthetic data, as well as process data from a simulated distillation column to validate its applicability and effectiveness in addressing safety concerns in the process industry. Finally, concluding remarks and future directions for research are presented.

Univariate Process Monitoring

Since this work focuses on extending the computationally simple Shewhart using multiscale representation, a brief overview of statistical and univariate process monitoring is needed. Most industries collect readings of process measurements through the utilization of multiple sensors. These sensors can monitor a number of different variables, such as temperature and pressure, to ensure that they are within acceptable limits for the purposes of plant safety and product quality. Univariate process monitoring methods can be implemented by following the algorithm illustrated in Figure 1.

As illustrated through Figure 1, process measurements collected from the sensors are initially compared to their model predictions (or desired values), creating process residuals. The process residuals are then used to compute a detection statistic. For the case of the Shewhart chart, the detection statistic is the process residuals themselves. For other univariate charts, such as the CUSUM or EWMA charts, the appropriate filter is applied in order to compute their respective detection statistics [28]. Using the distribution of the detection statistic, control limits (that can be used to determine the presence of absence of faults) can be computed. To test if new process measurements are faulty, the detection statistic is computed once again using the process residuals from testing data, which is then compared to these control limits. If the detection statistics computed from the testing data violate the control limits, a fault is declared. If the control limits are not violated by the detection statistic, the process is assumed to be operating under normal operating conditions, and no action is required.

For the Shewhart chart, the upper and lower fault detection control limits may be computed as follows [28]:

$$UCL, LCL = \mu_0 \pm 3\sigma \tag{1}$$

Where, μ_0 and σ are the mean and standard deviation of the detection statistic (which is the residuals for the Shewhart chart) obtained under normal operating conditions, respectively. The 3σ limits are commonly used for the Shewhart chart as they account for nearly 99.74% of all deviations in the data [29]. As stated previously,

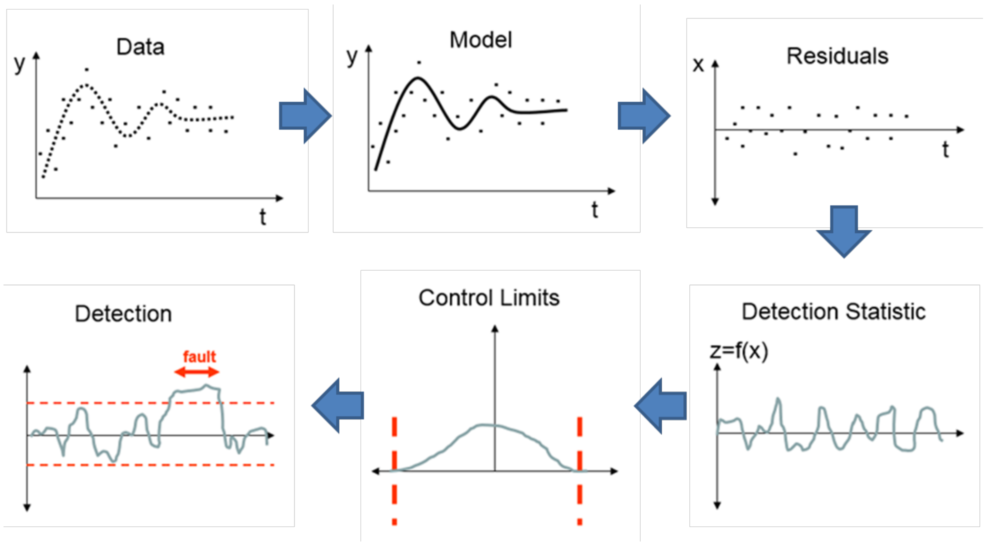

Figure 1: Algorithm for univariate process monitoring.

multiscale representation can help deal with violation in assumptions of most univariate monitoring methods. In the next section, multiscale wavelet-based representation of data is introduced, its advantages in fault detection are discussed, and a method to utilize these advantages to improve the effectiveness of the Shewhart chart is presented.

Multiscale Wavelet-Based Representation of Data

Practical process data, especially those collected from industrial processes are known to possess multiscale characteristics, i.e., they may contain noise or features that span wide ranges in both the frequency and time domains. For example a sharp change in the process data may span a narrow range in the time domain while spanning a much larger range in the time domain. Similarly, a slower change in the process data may span a wide range in the time domain, and a narrow range in the frequency domain [30]. Unfortunately, most commonly employed fault detection techniques in the process industry only operate on a single scale since they are applied on the time domain data, and therefore are unable to efficiently account for process data that may be multiscale in nature.

Multiscale wavelet-based representation of data is a powerful tool that has been used in data analysis. It is able to provide efficient separation of deterministic and stochastic features [31], and it has been successfully used to improve the accuracy of various process modeling, filtering, and state estimation techniques [32-34]. In multiscale representation, wavelet and scaling basis functions, which have the following form are used to represent time-domain functions and data at multiple resolutions and scales [35,36]:

$$\theta(t) = \frac{1}{\sqrt{s}}\theta\left(\frac{t-u}{s}\right) \tag{2}$$

where, the dilation and translation parameters are represented by s and u, respectively. A variety of families of basis functions have been used to carry out wavelet decomposition, e.g., Daubechies and Haar [37-39]. Several researchers utilized the Haar wavelet in various applications, and it will be utilized in the examples presented in this work [35,39,40]. Given a time domain data set (or a signal), a coarser approximation of the signal (often called a scaled signal) can be obtained by convoluting the original signal with a low pass filter h, which is derived from a scaling basis function of the following form [41]:

$$\phi_{ij}(t) = \sqrt{2^{-j}}\phi\left(2^{-j}t-k\right) \tag{3}$$

where, the dilation and translation parameters are represented by j and k, respectively. The difference between the original signal and the scaled signal is the detail signal, and can be obtained by convoluting the original and subsequent scaled signal with a high pass filter g, which is derived from a wavelet basis function of the following form [41]:

$$\psi_{ij}(t) = \sqrt{2^{-j}}\psi\left(2^{-j}t-k\right) \tag{4}$$

After repeating these approximations, the original signal can be reconstructed by taking the sum of the final scaled signal and all detail signals, as follows [41]:

$$x(t) = \sum_{k=1}^{n2^{-J}} a_{Jk}\phi_{Jk} + \sum_{j=1}^{J}\sum_{k=1}^{n2^{-J}} d_{jk}\psi_{jk}(t) \tag{5}$$

A number of researchers have utilized multiscale wavelet-based representation of data to improve fault detection. For example, [40] used multiscale representation to pre-filter the data, and then applied Principal Component Analysis (PCA) using the pre-filtered data. Pre-filtering of the raw data, before employing a fault detection technique, improves the effectiveness of the approach. However, pre-filtering may remove features in the data that are important for fault detection. Multiscale representation of data has also been used to develop a multiscale PCA (MSPCA) algorithm with improved performance over the conventional PCA method [35]. This is primarily due to multiscale being able to efficiently separate feature from noise making the MSPCA algorithm more sensitive to anomalies in process measurements than the conventional one. On the other hand, the performances of the many conventional univariate monitoring techniques have been limited by their inability to efficiently handle violations in their fundamental assumptions, like the presence of measurement noise, autocorrelation, as well as non-normality of evaluated residuals. Dealing with these limitations will help satisfy the assumptions of the various univariate fault detection techniques, which will reflect on their performances. Multiscale representation is an effective tool that is able to help deal with these challenges and its advantages are described in the next section.

Advantages of multiscale wavelet-based data representation

Ability to separate features from noise: A main assumption of the Shewhart chart is that the process data contains a moderate level of noise. One main benefit of multiscale representation is its ability to naturally separate noise from important features that may be present in the process data, which can be helpful from a fault detection perspective. This characteristic can be attributed to the successive application of high and low pass filters on the data in multiscale decomposition as illustrated in Figure 2. The noise-feature separation characteristic of multiscale representation and its advantages over other conventional linear filtering methods have been utilized in various applications, such as filtering time-series genomic data [41]. In this work, this separation ability of multiscale representation will also be employed in order to improve the performance of the conventional Shewhart chart, to widen its applicability in practice.

Ability to decorrelate autocorrelated data at multiple scales: Another fundamental assumption of the Shewhart chart is that the evaluated residuals are independent or uncorrelated. An important advantage of multiscale representation is that the wavelet coefficients obtained in multiscale decomposition are approximately decorrelated at multiple scales [42]. This can be illustrated by comparing the autocorrelation function (ACF) of an autocorrelated signal to the ACF of its details signals at multiple scales. The ACF, which plots the correlation between any two samples in a data set as a function of their separation, is usually used to quantify the autocorrelation in the data [43]. ACF measures the stochastic process memory in the data. Therefore, a white noise signal (which has independent samples) will have an autocorrelation function of zero for positions of lags other than zero, and a value of unity at lag zero, which indicates that the data set consists of completely uncorrelated samples. Conversely, correlated signals, such as those represented by autoregressive (AR) or autoregressive moving average (ARMA) models have non-zero ACF values at lags other than zero, which indicates that there is autocorrelation in the data [42]. To illustrate this characteristic, autocorrelated data are generated using the following AR (1) model [43]:

$$x_t = a x_{t-1} + \varepsilon \tag{6}$$

where, $a = 0.7$ *and* ε is white noise following a standard normal distribution with zero mean and unit variance. The obtained data are then decomposed at multiple scales and the ACF is computed for the time domain data as well as for all detail signals as shown in Figure 3. The first column of Figure 3 shows the time domain and detail signals, while the second column shows the ACF for all signals. Figure 3a clearly shows that, even though the time domain data are strongly correlated as indicated by the ACF shown in Figure 3b, the detail signals are approximately decorrelated at multiple scales as indicated by their ACFs shown in Figures 3c-3h. The decorrelation of detail signals at multiple scales can be attributed to the application of high-pass filters during wavelet decomposition [42].

Ability to better follow a normal distribution at multiple scales: The Shewhart chart also assumes that process residuals obtained from fault-free data follow a normal distribution. In practice, measured data may not necessarily follow a normal distribution. Modeling errors that leave non-modeled process variations in the model residuals can also be a source of non-Gaussian errors. Fortunately, multiscale decomposition is able to help address the issue of non-Gaussian errors as it provides detail signals that are closer to normal (Gaussian) at different scales.

To illustrate the effect of multiscale representation of data on the distribution of the detail signals, histograms of a chi square distributed data set and the detail signals obtained from its multiscale decomposition are compared as shown in Figure 4. Figure 4a shows that, even though the distribution of the time domain data is far from normal (which is expected since they follow a chi- square distribution) as indicated by Figure 4b, the histograms of the detail signals are closer to normality as indicated by Figures 4c-4h. Distributions other than chi-square were also used to validate this observation [30,44].

Furthermore, it should be noted that the multiscale representation provides wavelet coefficients that are also closer to being stationary for non-stationary data [24,35]. In this section, it has been shown that multiscale representation possesses advantages that can help

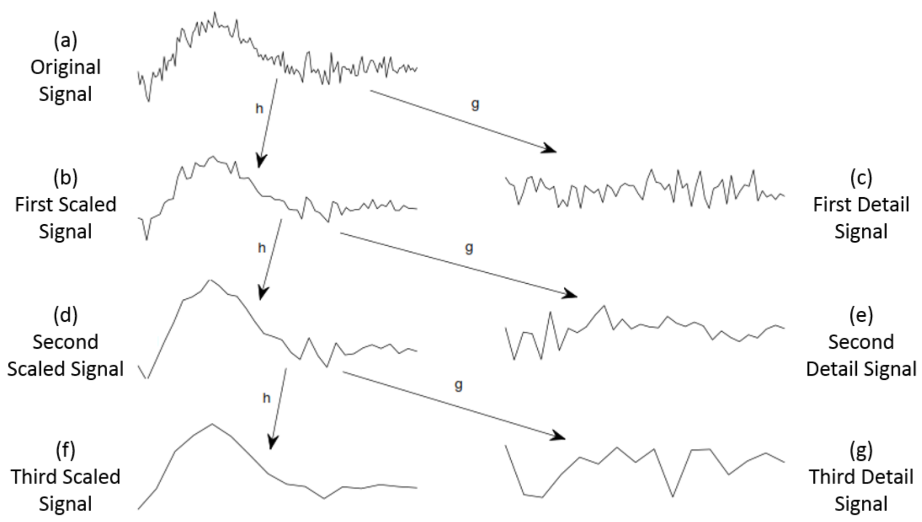

Figure 2: Schematic illustration of multiscale wavelet-based representation of data.

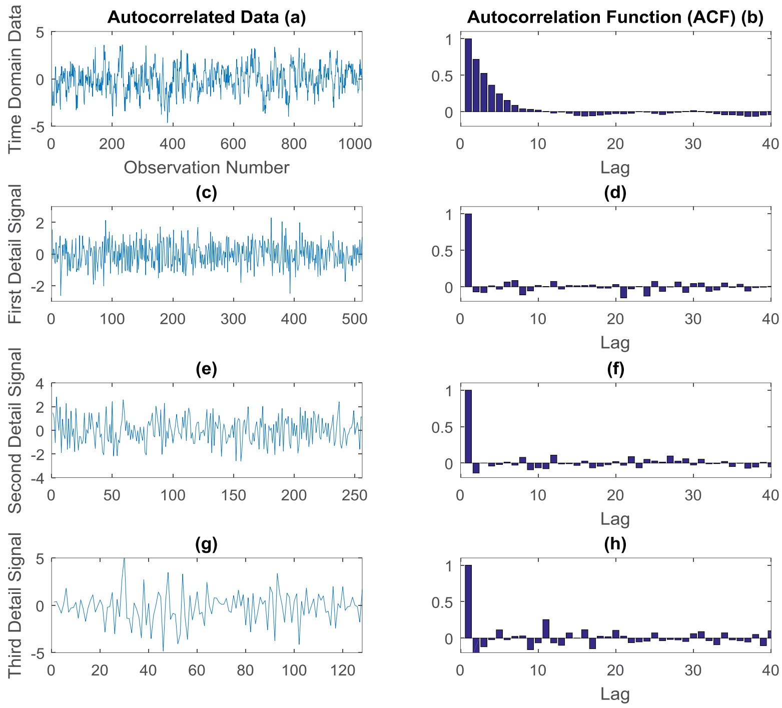

Figure 3: Decorrelating auto correlated data at multiple scales.

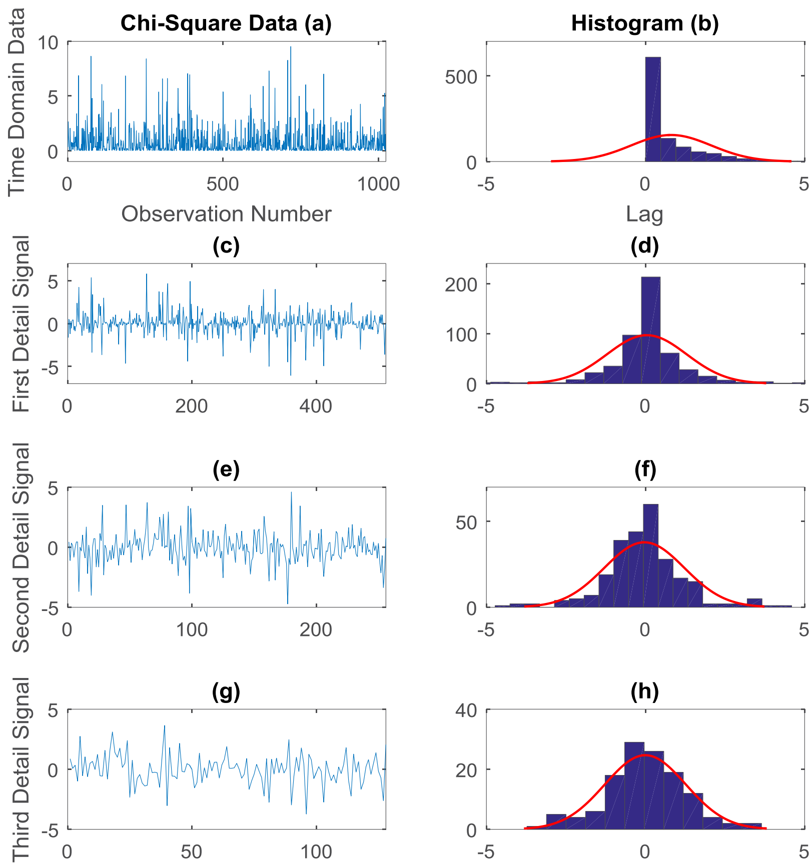

Figure 4: Distribution of chi-square data becomes Gaussian at multiple scales.

address many of the limitations that hinder the wide applicability of the Shewhart chart in practice. These advantages brought forward by multiscale representation are employed in this work to develop a multiscale Shewhart chart algorithm, which is described next.

Multiscale Shewhart chart fault detection algorithm

This section presents a multiscale Shewhart chart algorithm that can be used to provide improved performance over the conventional Shewhart chart. The idea behind this algorithm is to apply the conventional Shewhart using the detail signals as well as the final scaled signal obtained from the multiscale wavelet-based decomposition [45,46]. The algorithm consists of two phases, training and testing, as illustrated in Figure 5. In the first phase (training), fault-free training data are decomposed at multiple scales. The Shewhart chart is then applied using the detail signals at different scales and the final scaled signal, during which the control limits at each scale are computed (these limits will be used later in the testing phase). These control limits are used to threshold the wavelet coefficients (the detail signals) at each scale and the final scaled signal, and for any scale where any violation of limits is detected, all wavelet coefficients from that scale are retained. All retained signals are then reconstructed, and the Shewhart chart is applied once again on the reconstructed data set, where the control limits are computed once again. In the second phase (testing), the data are again decomposed at multiple scales (using the same wavelet filter utilized during the training phase). The control limits computed for each scale from the training phase are applied to the detail signals (and final scaled signal) for the testing data, and only the retained coefficients (after thresholding) are used to reconstruct the data set back in the time domain. Finally, the control limits obtained from the reconstructed training data are applied to the reconstructed testing data in order to detect any possible faults. This multiscale Shewhart chart algorithm is schematically represented in Figure 5.

It is important to note that for the wavelet reconstruction phase of the multiscale Shewhart fault detection algorithm, there are theoretically four alternative methodologies that can be used when deciding how to retain wavelet coefficients that violate the threshold limits at a particular scale [47]:

1. Retaining the entire scale of wavelet coefficients for both the training and testing data sets.
2. Retaining the entire scale of wavelet coefficients for the training data set, but only retaining the wavelet coefficients from each scale for the testing data set.
3. Retaining only the wavelet coefficients from each scale for both the training and testing data sets.
4. Retaining only the wavelet coefficients for the training data set, but retaining the entire scale of wavelet coefficients for the testing data set.

Methodology 2 was selected for the fault detection algorithm for the following reasons:

- Retaining the entire scale of wavelet coefficients during the training phase of the algorithm increases the number of observations available in the reconstructed training data set. This is particularly important from a fault detection perspective for the multiscale Shewhart chart, as a larger number of observations in the reconstructed training data set will give a more accurate estimation of the true standard deviation of the data. Retaining the entire scale of wavelet coefficients for scales that violate the threshold limits has the added advantage of only retaining scales that have important features and disregarding scales that do not contribute important features to the data set, thus acting similar to a filter.
- Since the standard deviation of the reconstructed data set is not an issue for the testing data, and we are only concerned with capturing faulty observations, retaining an entire scale when a threshold limit violation occurs is not necessary. If a fault is present in the testing data set, the final scaled signal will be able to detect the fault accurately, and reconstructing only coefficients that violate the threshold limits will show up as a clear pulse in the reconstructed testing data set, thereby violating the fault detection limits of the multiscale Shewhart chart.

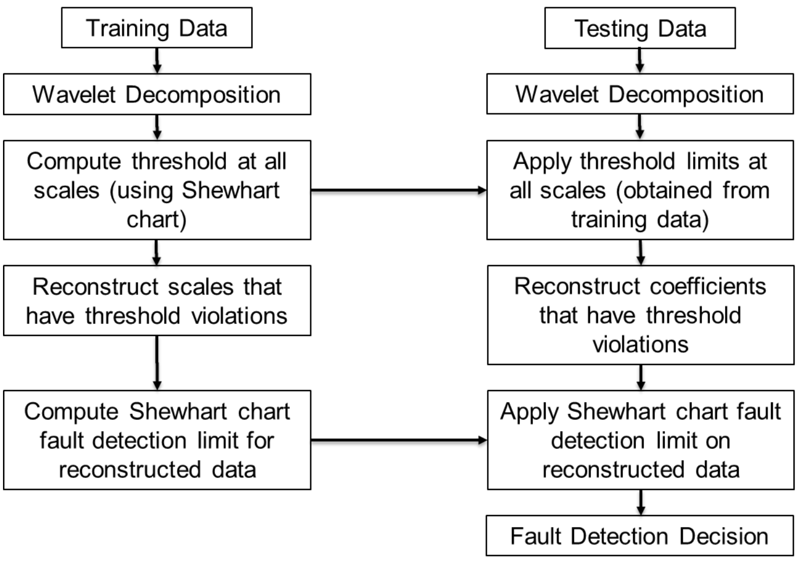

Figure 5: Schematic illustration of the developed multiscale Shewhart chart fault detection algorithm.

Citation: Sheriff MZ, Nounou MN (2017) Improved Fault Detection and Process Safety Using Multiscale Shewhart Charts. J Chem Eng Process Technol 8: 328. doi: 10.4172/2157-7048.1000328

Illustrative Examples

This section compares the performance of the developed multiscale Shewhart chart to that of the conventional one using two illustrative examples: using synthetic data and using process data generated from a simulated distillation column. The simulated synthetic example examines the performance of both charts using data generated under a variety of conditions, in order to examine the robustness of the developed Shewhart chart, especially when the fundamental assumption of the conventional chart are violated.

Performance assessment under different levels of noise

Process data are usually contaminated with errors or noise. An essential feature of any monitoring technique used in the process industry is that it needs to be able be able to handle process data that are contaminated with noise, since it can severely deteriorate the performance of the technique. The higher the noise level, the more challenging it becomes to distinguish the difference between random variations in the process and faults. Therefore, this section examines the performance of both Shewhart charts at different noise levels.

In order to carry out this assessment, training data (consisting of 512 observations) that follow a standard normal distribution (of zero mean and unit variance), is used to compute the fault detection limits of both charts. Similarly, testing data (consisting of 512 observations) is generated, with additive steps faults of ± 3 added at two locations between observations 101-150 and 401-450, respectively. The simulation is then repeated using different noise standard deviations (σ=0.01- 5). This wide range of noise allows assessing the robustness of both charts to the presence of noise. A Monte-Carlo simulation of 5000 realizations is carried for each level of noise to ensure that accurate results are obtained and meaningful conclusions can be drawn. At each noise level, the performance of both charts are assessed by computing three fault detection metrics: missed detection rate (%), false alarm rate (%), and out-of-control average run length (ARL_1). Examining the performance of both charts, utilizing all three metrics allows us to assess their advantages and limitations.

The results of missed detection and false alarm rates for both charts are illustrated in Figure 6. These results show that even though the noise level does not change the false alarm rate, the missed detection rate increases at higher noise levels and can reach nearly 100% for very high levels of noise. Furthermore, it can also be seen that the false alarm rates are comparable for both techniques, and that the missed detection rate is consistently lower for the multiscale method than the conventional method. This can be attributed to the noise-feature separation characteristic of the multiscale method highlighted previously. with improve the detection ability of the Shewhart chart providing a reduction in missed detection rate of approximately 40% for certain noise levels.

The ARL_1 results on the other hand, are illustrated in Figure 7. These results show that for low to moderate levels of noise (σ=0.01-2), the conventional method provides comparable or slightly lower ARL_1 values than the multiscale method. However, for higher levels of noise (σ=2-5), it is evident that the multiscale method provides much lower ARL_1 values, which are due to the noise-feature separation advantage of multiscale representation, especially at high noise levels. The advantage of using the multiscale Shewhart chart over the conventional one when dealing data that are contaminated with noise can be further demonstrated by comparing the time series evolutions of the two charts at different levels of noise as illustrated in Figure 8. The results shown in Figure 8 demonstrate that at low noise levels, e.g., 0.5, the performances of both charts are comparable, with both charts achieving nearly 100% detection see Figures 8a and 8b. However, at moderate levels of noise, e.g., σ=2.5, the multiscale Shewhart outperforms the conventional one with much better detection (Figures 8c and 8d). At even higher noise levels, e.g., σ=4.5, the multiscale Shewhart chart shows even better fault detection abilities and even quicker detection (i.e., smaller ARL_1) as shown in Figures 7, 8e and 8f. These results clearly show that when process measurements are contaminated with noise, utilizing the multiscale Shewhart chart results in faster fault detection (lower ARL_1), which would allow quicker response thereby increasing the chance of averting any catastrophic disasters.

Performance assessment under different levels of autocorrelation

The second main assumption of the Shewhart chart is that the

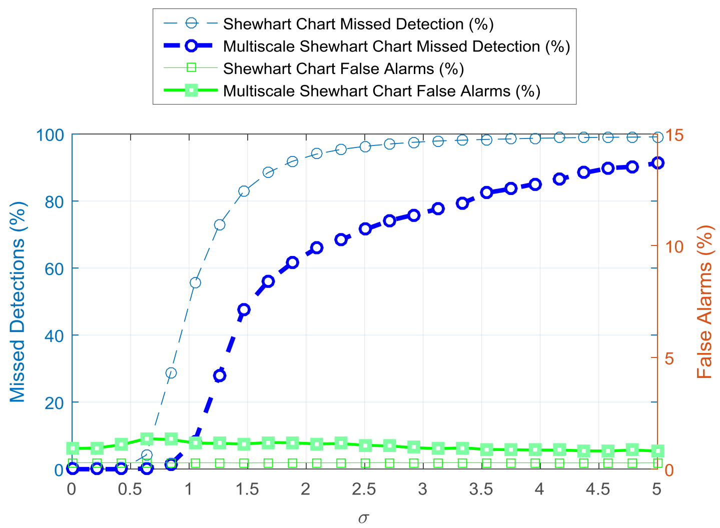

Figure 6: Performance comparison for the conventional and multiscale Shewhart charts for different noise levels (Missed Detection and False Alarm rates).

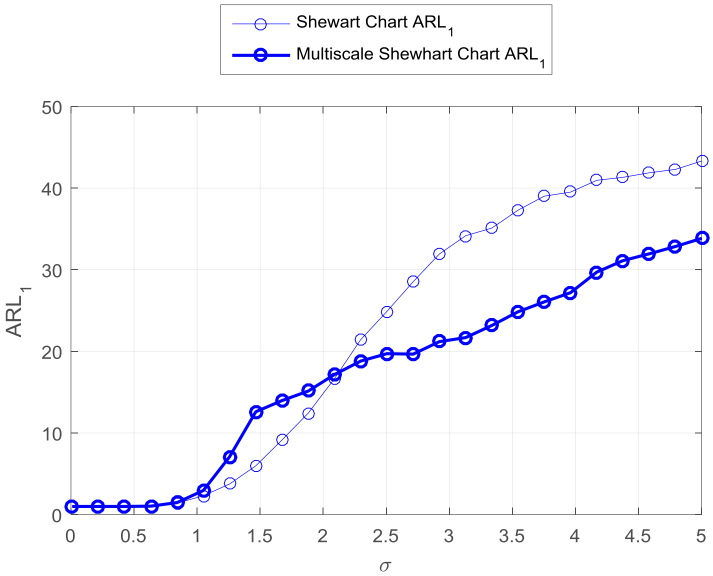

Figure 7: Performance comparison of the conventional and multiscale Shewhart charts for different noise levels (ARL_1).

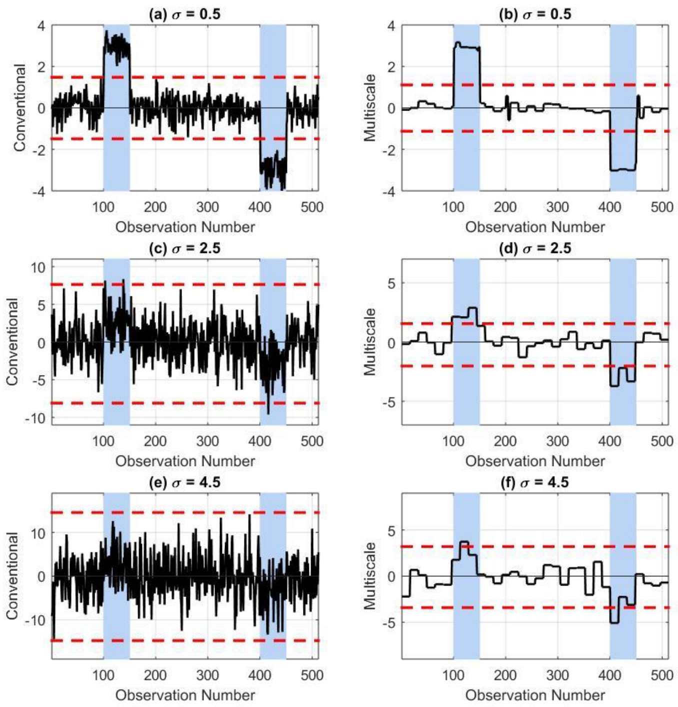

Figure 8: Time evolution comparison of the conventional and multiscale Shewhart charts for different noise levels.

process residuals being evaluated are uncorrelated (consecutive observations are independent). In practice, however, this assumption may not hold due to possible modeling errors or malfunctioning sensors that introduce correlation between consecutive observations, which can greatly affect the performance of the Shewhart chart. As described previously, multiscale, multiscale representation helps decorrelate autocorrelated data, which should provide the multiscale Shewhart chart an advantage when dealing with autocorrelated process measurements. This section presents a comparison and an assessment of the performances of both charts at different degrees of autocorrelation.

In order to carry out this assessment, an autoregressive AR (1) model (Equation 6) is used to generate training data (consisting of 512 observations). Similarly, testing data (consisting of 512 observations) are generated, but with additive step faults of magnitude 3 added at two locations between observations 101-150 and 401-450, respectively.

Then, the conventional and multiscale Shewhart charts are used to detect these faults. To provide a thorough assessment of the effect of autocorrelation and the robustness of both charts to autocorrelated data, the simulation is repeated for a wide range of autocorrelation (a = 0.01-0.99). Once again, a Monte-Carlo simulation of 5000 realizations is carried out for each level of autocorrelation, to ensure that accurate results are obtained and meaningful conclusions can be drawn.

The results of the simulation for both charts with regards to the missed detection and false alarm rates are illustrated in Figure 9. As Figure 9 demonstrates, although both charts show that the false alarm rate remains relatively constant (except at extremely high values of autocorrelation), the missed detection rate increases (to nearly 100%) as the degree of autocorrelation increases for both charts. Even though the false alarm rates are comparable for both charts, the missed detection rates obtained by the multiscale Shewhart chart are consistently lower than those obtained by the conventional chart (providing nearly 40% lower values of missed detection for a wide range of autoregressive coefficient). This advantage of the multiscale method is due to the ability of multiscale representation to decorrelate data at multiple scales as described in Section 3.1.3. Furthermore, Figure 10 that illustrates the ARL_1 values for both charts, shows that they provide comparable values over the entire range of autoregressive coefficient. This means that even though the multiscale Shewhart chart provides a better missed detection rate, it does not provide clear advantages in terms of the speed of detection.

The advantage of using the multiscale Shewhart chart over the conventional one when dealing when data that are autocorrelated, can be further demonstrated by comparing the time series evolutions of the charts at different levels of autoregressive coefficient as illustrated in Figure 11. The results illustrated in Figure 11 show that the multiscale Shewhart chart outperforms the conventional one at low and moderate autocorrelation levels (i.e., *a*=0.1 and *a*=0.5) as illustrated in Figures

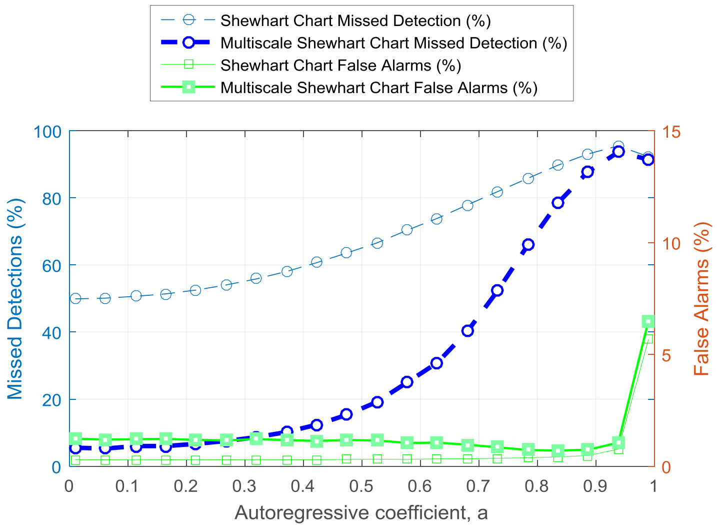

Figure 9: Performance comparison for the conventional and multiscale Shewhart charts for different autocorrelation levels (Missed Detection and False Alarm rates).

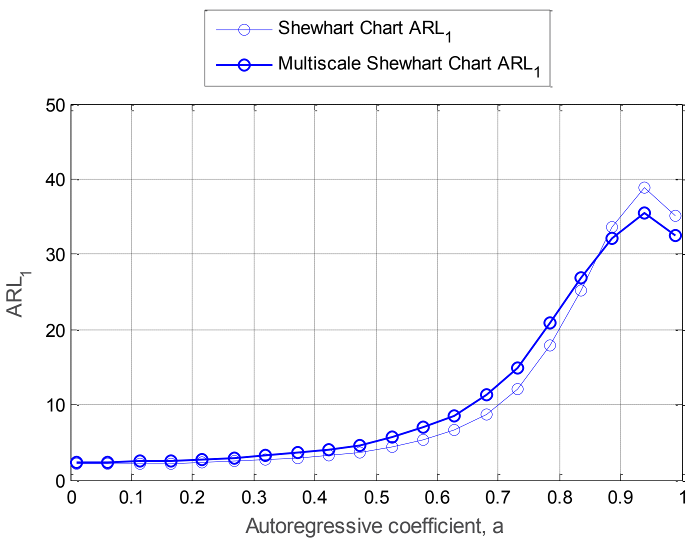

Figure 10: Performance comparison for the conventional and multiscale Shewhart charts for different autocorrelation levels (ARL_1).

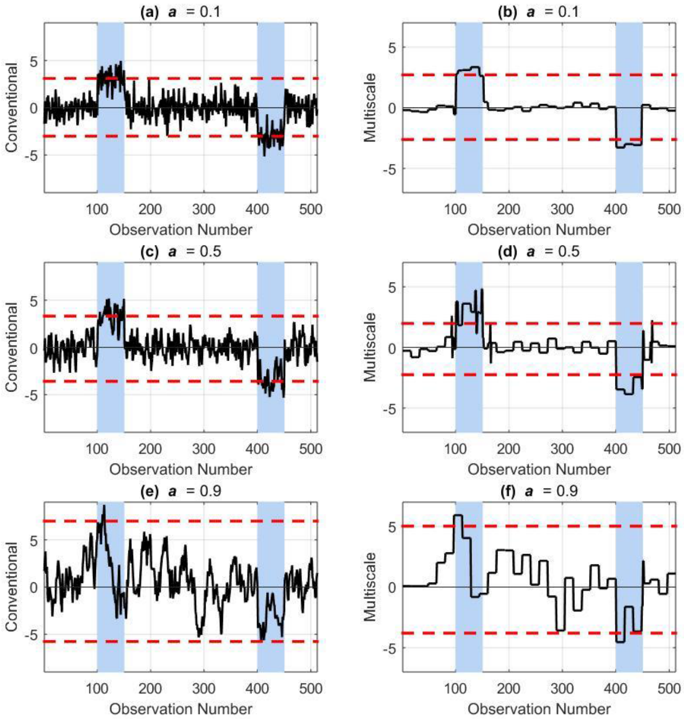

Figure 11: Time evolution comparison of the conventional and multiscale Shewhart charts for different autocorrelation levels.

11a and 11b for the case of a 0.1 and in Figures 11c and 11d for the case of a=0.5. At very high level of autocorrelation, however, as in the case where a=0.9, both charts fail to properly detect both faults in the data as illustrated in Figures 11e and 11f. This very high of autocorrelation is not very commonly encountered in practice, which makes the multiscale technique applicable in most practical situations. Therefore, utilizing the developed multiscale Shewhart when dealing with autocorrelated data is advantageous. Even though the response time is comparable (similar ARL_1 values) for both techniques, the multiscale chart is able to provide significantly lower missed detection rates over a wide range of autocorrelation coefficient, proving to be more robust that the conventional chart.

Performance assessment with distributions of varying degrees of non- normality

The third main assumption of the Shewhart chart is that it assumes that the fault-free process residuals being evaluated follow a Gaussian (normal) distribution. Practical data, however, might not always satisfy this assumption, thereby degrading the performance of the Shewhart chart. This section assesses and compares the performances of both charts under violation of this assumption. In practice, non-Gaussian noise can be a result of malfunctioning sensors, which introduce a certain bias or skewed randomness to the process observations being monitored. Non-Gaussian noise may also be introduced to the data by modeling errors that leave non-modeled process variations in the model residuals. Therefore, this assumption also needs to be dealt with in order to carry out efficient and safe process monitoring. To assess the effect of the distribution on the quality of fault detection, distributions of different degrees of non-normality are needed, along with a metric to quantify the level or degree of normality. A chi-square distribution can be utilized for this purpose in order to obtain data sets with different degrees of normality. The chi square distribution has the following probability density function [29]:

$$f(x) = \frac{1}{2^{\frac{k}{2}}\Gamma(\frac{k}{2})} x^{\frac{k}{2}-1} e^{-\frac{x}{2}} \tag{7}$$

where, k represents the number of degrees of freedom. Adjusting the parameter k produces distributions with different degrees of normality. There are a number of metrics that can be utilized to test the normality of a given distribution. The Shapiro-Wilk metric is often considered to be one of the most powerful univariate normality tests [44], and hence it is used in this work to quantify the deviation from normality. The Shapiro-Wilk metric varies from zero to one, where a value closer to one implies that the distribution is closer to normality, and vice versa. Further detail on the Shapiro-Wilk and other metrics commonly used to quantify the deviation from normality can be found in [30,44]. In order to perform this assessment, the chi-square distribution is used to generate training data (consisting of 512 observations), which are used to compute the control limits for both charts. Testing data are also generated in a similar manner, and additive step faults of magnitude ±3σ (where σ is the standard deviation of the generated training data) are added at two locations between observations 101-150 and 401-450, respectively. For this simulation it is important to generate the faults with opposite signs (one positive and one negative) in order to ensure that effect of the direction (bias) of skewness in the non-Gaussian distribution is eliminated when assessing both techniques. To examine the performance of both charts at different levels of non-normality, this simulation is repeated for a wide range of Shapiro-Wilk values (between approximately 0.75-0.99). Once again, a Monte-Carlo simulation of 5000 realizations is carried out for each value of Shapiro-Wilk, to ensure that accurate results are obtained and meaningful conclusions can be drawn. The results of the simulation for both charts with regards to the missed detection and false alarm rates are illustrated in Figure 12.

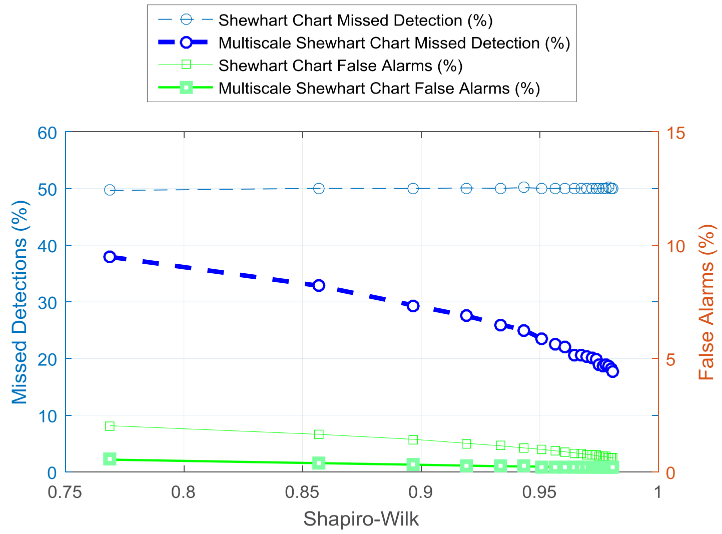

Figure 12: Performance comparison for the conventional and multiscale Shewhart charts for different cases of non-normality (Missed Detection and False Alarm rates).

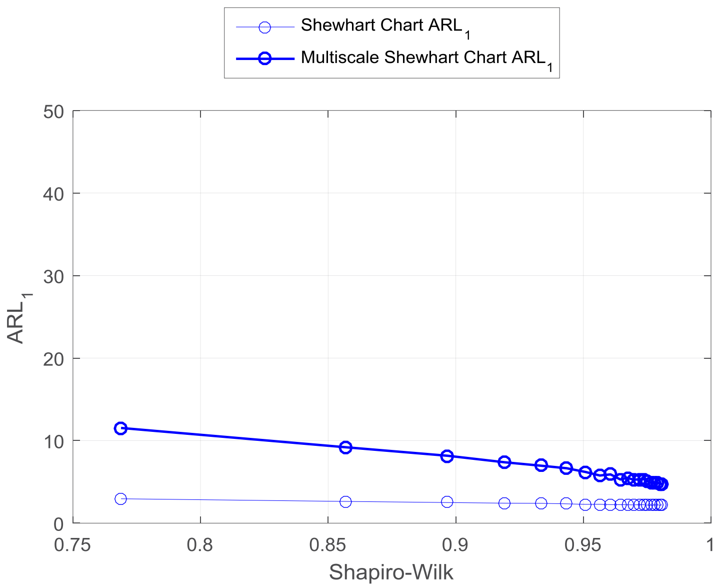

Figure 13: Performance comparison for the conventional and multiscale Shewhart charts for different cases of non-normality (ARL_1).

Figure 12 demonstrates that, for both charts, the missed detection and false alarm rates remain relatively constant at different degrees of non-normality. This will be explained and visually illustrated later in Figure 14. Figure 12 also shows that even though the false alarm rates are somewhat comparable for both charts, the missed detection rates for the multiscale methods are consistently better than the conventional method (with a reduction of nearly 30%) in the missed detection rate at some values of Shapiro-Wilk). These results can be attributed to the fact that multiscale representation provides detail signals that are approximately Gaussian at multiple scales even for non-Gaussian data [48]. On the other hand, Figure 13, that compares the ARL_1 for both charts, shows that even though the multiscale Shewhart chart provides a better detection rate, it is unable to provide lower ARL_1 values than the conventional chart, especially at lower values of Shapiro-Wilk. However, it should be noted that this increase in ARL_1 for the multiscale Shewhart chart is for data which deviate considerably from normality, which is not very common in practice. This issue may be remedied by fine-tuning the decomposition depth of the multiscale technique to ensure that both techniques provide similar ARL_1 values. An analysis of the choice of decomposition is presented in the upcoming section.

The advantage of using the multiscale Shewhart chart over the conventional one when dealing with data that deviate from normality, can be further demonstrated by comparing the time series evolutions of the charts at different degrees of deviation from normality (values of Shapiro-Wilk) as illustrated in Figure 14. These results indicate that even when the data are approximately normal, the multiscale Shewhart chart is able to outperform the conventional one, providing a reduction in the missed detection rate of nearly 30%. This advantage can also be seen for higher deviations from normality (i.e., for Shapiro-Wilk=0.87

and 0.75), but with narrow margins as illustrated in Figure 14c and 14d for the case of a moderate deviation from normality (Shapiro-Wilk=0.85) and in Figures 14e and 14f for the case of a high deviation from normality (Shapiro-Wilk=0.75). Additionally, it is important to note that the performance of the Shewhart chart is not highly affected by the deviation from normality of the data. This can be explained as follows: as the distribution of the data starts deviating from normality, the data becomes increasingly one-sided, and the control limits adjust to the direction of the distribution, which causes the performance of the conventional Shewhart chart to remain relatively constant over a wide range of non-normality as illustrated in Figure 14.

Effect of decomposition depth

An important decision when it comes to implementing the multiscale Shewhart chart in practice is the choice of decomposition depth, i.e., the number of scales to be used in the wavelet decomposition of the data. This section studies the effect decomposition depth has on the performance of the developed multiscale Shewhart chart. This analysis is performed by first generating training data (consisting of 512 observations) using a standard normal distribution (having zero mean and unit variance), which are then used to compute the control limits of the chart. The testing data are generated in a similar manner, and additive step faults of magnitude ±3σ are introduced at two locations between observations 101-150 and 401-450, respectively, where σ represents the standard deviation of the training data set. This simulation is repeated for different decomposition depths, and a Monte-Carlo simulation of 5000 realizations is run for each decomposition in order to obtain accurate results and to draw meaningful conclusions. As with the previous examples, the performance of the chart is evaluated

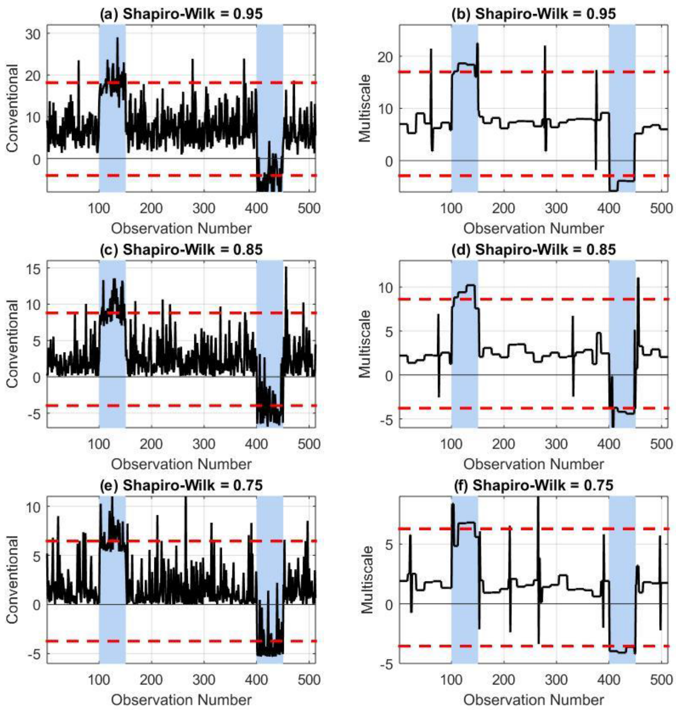

Figure 14: Time evolution comparison of the conventional and multiscale Shewhart charts for cases of non-normality.

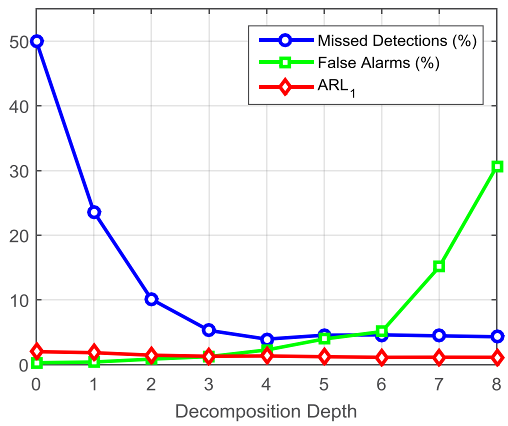

Figure 15: Analysis of the effect of choice of decomposition on the performance of the multiscale Shewhart chart.

Citation: Sheriff MZ, Nounou MN (2017) Improved Fault Detection and Process Safety Using Multiscale Shewhart Charts. J Chem Eng Process Technol 8: 328. doi: 10.4172/2157-7048.1000328

using all three fault detection metrics. The mean value of all three metrics is computed from all 5000 realizations at each decomposition depth and the results are shown in Figure 15. The results show that the missed detection rate decreases as the number of scales increases, but up to a certain scale after which it settles to an almost constant value. Conversely, the false alarm rate increases as the number of scales increases. These observations are due to the fact that at coarser scales, more noise is removed and features are better detected, which decreases the missed detection rate. Also, at coarser scales, the control limits get tighter and tighter, which results in all the detail coefficients being retained. This would therefore not add any further detection advantage, but results in a slight increase in the false alarm rate. Figure 15 also shows that the ARL_1 is not greatly affected by the choice of decomposition depth. Therefore, in this example, an optimum depth of four can be selected. From practical experience, a depth of around half of the maximum possible decomposition depth is recommended.

Monitoring of a simulated distillation column using the Multiscale Shewhart chart

Although the illustrative examples presented thus far have made a strong case for using the developed multiscale Shewhart chart especially when dealing with process data that violate the assumptions of the conventional method, it is essential to examine how the charts perform in a practical situation. This section provides such an example where the performance of both Shewhart charts are assessed by applying them using process data from a simulated distillation column. Separation processes are a crucial part in many chemical plants, and distillation columns are often among the most commonly used separation units. The operation of distillation columns needs to be monitored to ensure that quality of products in the different streams meet the sought standards, and to ensure that the process is running safely.

It is possible for explosions to occur at distillation columns, if improper monitoring measures are in place. One such example is an explosion that took place on July 30, 2000, at a manufacturing company that produces specialty gases located in Dayton, NV. Although, no staff were injured at the facility, the building structure that housed the equipment was severely damaged [49]. The incident occurred in the distillation column that was used to separate residual fluorine and nitrogen gas from condensed nitrogen trifluoride. The incident occurred because the facility received liquid nitrogen that was much cooler than the nitrogen stored at the facility. The liquid nitrogen was used as a coolant in the heat exchanger and the colder temperature of the coolant forced the fluorine to liquefy. The incident investigation report concluded that condensed fluorine had reactor with the packing material made of stainless steel, and had caused an exothermic reaction to occur inside the reboiler/condenser of the distillation column. Combustion between the steel material and liquid nitrogen trifluoride was initiated, and the energy that was released from the exothermic reactions caused pressure and temperature to build up in distillation column, leading to an eventual explosion [49]. Therefore, it essential for streams in the distillation column, and other equipment in industrial facilities to be continuously monitored efficiently, to ensure incidents such as these do not occur or are minimized and handled before leading to more catastrophic ones. In this example, Aspen Tech 7.2 was utilized in order to simulate distillation column data. The goal of the simulation was to monitor the distillate stream of the column. The distillation column consisted of 32 theoretical layers, including both a total condenser and a reboiler. The feed stream (which has a composition of 60 mole% isobutene and 40 mole% propane), enters the column at a flow rate of 1 kmol/s as a saturated liquid at at stage 16. The nominal operating conditions for this distillation column are provided in [50]. In order to generate dynamic data, the reflux and feed flow rates are perturbed from the nominal values at which they operate, and step changes (with magnitude ± 2%) are introduced to the feed flow rate. Once the process has settled to a new steady state, similar perturbations are introduced in the reflux flow rate, and it is allowed to settle to a new steady state. A data set of 1024 observations is generated, which consists of the temperatures at different trays and the compositions in the product streams. These data are assumed to be noise-free and therefore are contaminated with Gaussian noise of zero mean. From a fault detection perspective, the goal of the simulation is to monitor the propane composition in the distillate stream (x_D). It is essential that all streams in a chemical process meet the required

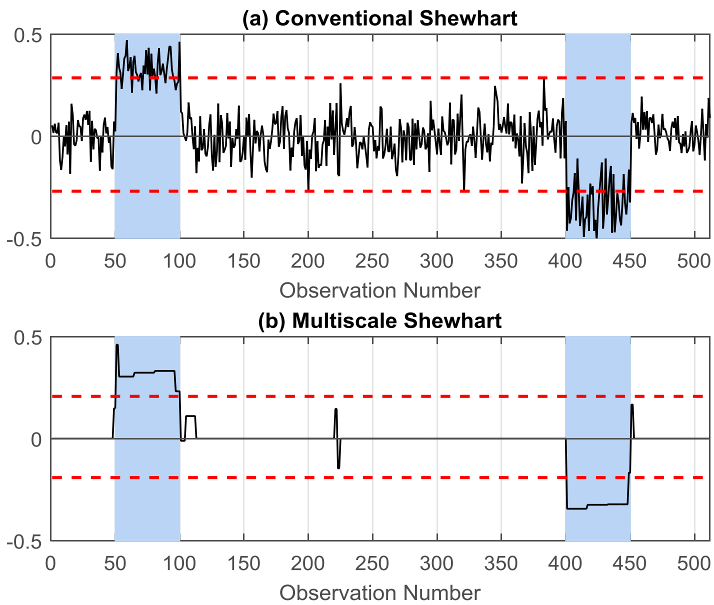

Figure 16: Comparison in performance of the conventional and multiscale Shewhart charts for a step fault of magnitude σ=3.5 in the process residuals.

specifications to avoid disastrous consequences.

The available process observations need to be compared to their reference values in order to compute the process residuals so that monitoring charts can be applied. A Partial Lest Squares (PLS) regression model was constructed and utilized in order to obtain the required process residuals. The process residuals are then split into two sets, 512 observations each, to be used as training and testing data sets. The training data are used to compute the fault detection (control) limits, which would then be utilized to detect faults in the testing data. Two step faults of magnitude ± σ 3.5 are added to the testing data at two locations between observations 51-100 and 401-450, respectively. Figure 16 illustrate the fault detection results for both the conventional Shewhart chart Figure 16a and the multiscale Shewhart chart Figure 16b. As demonstrated in Figure 16, the multiscale Shewhart chart is more able to detect the fault, with a significantly lower missed detection rate (~ 0%) when compared to the conventional Shewhart chart, which also detects most of the faults. Figure 16 also shows that the multiscale Shewhart chart does provide a lower false alarm rate when compared to the conventional chart.

The same simulation was also repeated for a step fault of magnitude ± 2.5 σ, again added between observations 51-100, and 401-450, respectively, and the results are illustrated in Figure 17. These results show that the conventional Shewhart chart is unable to detect most of the fault Figure 17a while the multiscale Shewhart provided nearly 100% detection. Figure 17 also shows that the multiscale Shewhart chart provides lower false alarm rates than the conventional one.

As illustrated through this simulated distillation column example, the developed multiscale Shewhart chart does outperform the conventional chart for two different magnitudes of step faults, as it is able to better detect the fault in both scenarios. Therefore, implementing the multiscale Shewhart chart for monitoring real chemical industries is advantageous.

Conclusion

Most univariate process monitoring techniques are known to rely on three main assumptions: that the process residuals are normally distributed, independent, and only contain moderate levels of noise. Data collected from sensors may violate one or more of these assumptions, which affects the performance of most univariate monitoring techniques. Multiscale representation has been shown to improve noise-feature separation in data, approximately decorrelate autocorrelated data, and transform data so that they better follow a normal distribution and multiple scales. In this work, these advantages of multiscale representation were utilized to enhance the performance of the Shewhart chart, through developing a multiscale Shewhart chart algorithm that can deal with these assumption violations. The multiscale algorithm relies on decomposing the data at multiple scales and applying the Shewhart chart using all detail signals and the last scaled signal, before being reconstructed back to the time domain. The performance of both charts, conventional and multiscale was then compared through simulated examples, in which the fundamental assumptions of univariate charts were violated at different levels using Monte-Carlo simulations. The performance was evaluated using three different criteria: the missed detection and false alarm rates, and as well as the out-of-control average run length, ARL_1. The results showed that the impacts of noise level and autocorrelation were most severe, as they led to missed detection rates of approximately 100% (at high levels of noise and autocorrelation) for the conventional chart. The impact of process residuals deviation away from normality was less critical. The results also showed that the multiscale technique was able to provide a reduction of approximately 40% in the missed detection rate over a wide range of noise levels, with a comparable false alarm rate, and lower ARL_1 than the conventional technique. The multiscale technique also provides a reduction of over 40% in the missed detection rate for a wide range of autocorrelation (except at high levels of autocorrelation) and lower ARL_1 values, while maintaining comparable false alarm rates, when compared to the conventional technique. Under violation of the normality assumption, however, the multiscale technique results in reductions in both the missed detection and false alarm rates for a wide range of non-normality, but in slightly higher ARL_1 values than those obtained by the conventional technique. The choice of decomposition

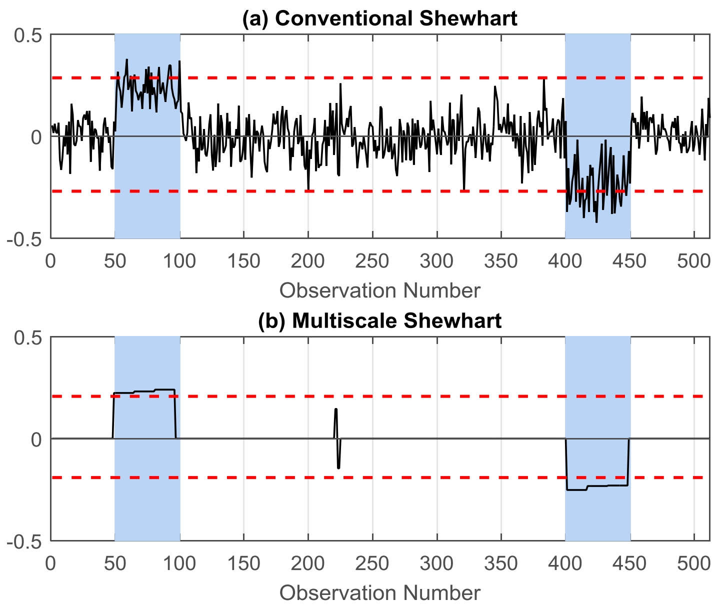

Figure 17: Comparison in performance of the conventional and multiscale Shewhart charts for a step fault of magnitude σ=2.5 in the process residuals.

depth is also an important factor in the implementation of the developed multiscale technique, and after evaluation of both charts using the three performance criteria for a range of decomposition depths, it was concluded that the optimal decomposition depth would generally be approximately half of the maximum possible decomposition depth for a given data set. The developed technique was additionally applied to a real world application, in which it is used to monitor the operation of a distillation column using simulated data. When used to monitor the distillate stream composition at two different fault sizes (2.5σ and 3.5σ), the multiscale approach was able to detect both faults with fewer missed detections and false alarms than the conventional technique. The relative computational simplicity of the proposed multiscale algorithm definitely encourages its implementation to improve process safety and product quality in a wide range of industrial processes. Although the developed algorithm does demonstrate significantly improved performance over the conventional technique, especially when the assumptions are violated, there are a few directions for future developments. The advantages obtained by the multiscale Shewhart chart algorithm can be extended to develop other univariate and multivariate multiscale monitoring techniques as well.

Acknowledgements

This work was made possible by NPRP grant NPRP7-1172-2-439 from the Qatar National Research Fund (a member of Qatar Foundation). The statements made herein are solely the responsibility of the authors.

References

1. Sarrate R, Aguilar J, Nejjari F (2007) Event-based process monitoring. Eng Appl Artif Intell 20: 1152-1162.
2. Venkatasubramanian V, Rengaswamy R, Yin K, Kavuri SN (2003) A review of process fault detection and diagnosis: Part I: Quantitative model-based methods. Comput Chem Eng 27: 293-311.
3. Venkatasubramanian V, Rengaswamy R, Yin K, Kavuri SN (2003) A review of process fault detection and diagnosis: Part II: Qualitative models and search strategies. Comput Chem Eng 27:313-326.
4. Nan C, Khan F, Iqbal MT (2008) Real-time fault diagnosis using knowledge-based expert system. Process Saf Environ Prot 86: 55-71.
5. Chetouani Y (2014) A sequential probability ratio test (SPRT) to detect changes and process safety monitoring. Process Saf Environ Prot 92: 206-214.
6. Rengaswamy R, Venkatasubramanian V (1995) A syntactic pattern-recognition approach for process monitoring and fault diagnosis. Eng Appl Artif Intell 8: 35-51.
7. Venkatasubramanian V, Rengaswamy R, Yin K, Kavuri SN (2003) A review of process fault detection and diagnosis: Part III: Process history based methods. Comput Chem Eng 27: 293-311.
8. Harrou F, Kadri F, Khadraoui S, Sun Y (2016) Ozone measurements monitoring using data-based approach. Process Saf Environ Prot 100: 220-231.
9. Yang Y, Liu Q, Gao Z (2015) Data fault detection in medical sensor networks. Sensors 15: 6066-6090.
10. Santos P, Villa LF, Reñones A (2015) An SVM-Based Solution for Fault Detection in Wind Turbines. Sensors 15: 5627-5648.
11. Martí L, Sanchez-pi N, Molina JM (2015) Anomaly detection based on sensors data in the petroleum industry applications. Sensors 15: 2774-2797.
12. Chakrabarty A, Mannan S, Cagin T (2015) Multiscale modeling for process safety applications. 1st edn. Butterworth-Heinemann.
13. US Chemical Safety Board (2007) Investigation Report Refinery Explosion and Fire. Chemical Safety and Hazard Investigation 341.
14. Shewhart WA (1930) Economic quality control of manufactured product. Bell Syst Tech J 9: 364-389.
15. Wang J, Luo C (2012) Long-period fiber grating sensors for the measurement of liquid level and fluid-flow velocity. Sensors 12: 4578-4593.
16. Page ES (1961) Cumulative Sum Charts. Technometrics 3: 1-9.
17. Roberts SW (1959) Control chart tests based on geometric moving averages. Technometrics 1: 239-250.
18. Hunter JS (1986) The exponentially weighted moving average. J Qual Technol 18: 203-210.
19. Cinar A, Undey C (1999) Statistical process and controller performance monitoring: A tutorial on current methods and future directions. Proc Am Control Conf, pp: 2625-2639.
20. Cinar A, Palazoglu A, Kayihan F (2007) Chemical Process Performance Evaluation. 1st edn. CRC Press, Boca Raton, FL, USA.
21. Cinar A, Parulekar SJ, Under C, Birol G (2003) Batch Fermentation. 1st edn. Marcel Dekker, Inc., New York, USA.
22. Cai L, Tian X (2013) A new fault detection method for non-Gaussian process based on robust independent component analysis. Process Saf Environ Prot 92: 645-658.
23. Lu CW, Reynolds MRJ (2001) CUSUM Charts for Monitoring an Autocorrelated Process. J Qual Technol 33: 316-334.
24. Ganesan R, Das TK, Venkataraman V (2004) Wavelet-based multiscale statistical process monitoring: A literature review. IIE Trans 36: 787-806.
25. Ganesan R (2007) Real-time monitoring of complex sensor data using wavelet-based multiresolution analysis. Int J Adv Manuf Technol 39: 543-558.
26. Reynolds MR, Stoumbos ZG (2004) Should observations be grouped for effective process monitoring? J Qual Technol 36: 343-366.
27. Guo H, Paynabar K, Jin J (2011) Multiscale monitoring of autocorrelated processes using wavelets analysis. IIE Trans 44: 312-326.
28. Montgomery DC (2013) Introduction to Statistical Quality Control. 7th edn. John Wiley & Sons, Hoboken, NJ, USA.
29. Montgomery DC, Runger GC (2011) Applied Statistics and Probability for Engineers. 5th edn. John Wiley & Sons Inc., Hoboken, NJ, USA.
30. Sheriff MZ (2015) Improved Shewhart chart using multiscale representation. Texas A&M University.
31. Mallat S (1989) A theory for multiresolution signal decomposition: the wavelet representation. Pattern Anal Mach Intell IEEE Trans II: 674-693.
32. Nounou MN (2006) Multiscale finite impulse response modeling. Eng Appl Artif Intell 19: 289-304.
33. Nounou HN, Nounou MN (2006) Multiscale fuzzy Kalman filtering. Eng Appl Artif Intell 19: 439-450.
34. Nounou MN, Nounou HN (2007) Improving the prediction and parsimony of ARX models using multiscale estimation. Appl Soft Comput 7: 711-721.
35. Bakshi B (1998) Multiscale PCA with application to multivariate statistical process monitoring. AIChE J 44: 1596-1610.
36. Davis J, Piovoso M, Hoo KA, Bakshi BR (1999) Process data analysis and interpretation. Adv Chem Eng 25: 1-103.
37. Daubechies I (1988) Orthonormal bases of compactly supported wavelets. Commun pure Appl Math XLI: 909-996.
38. Daubechies I (1992) Ten Lectures on Wavelets. Library of Congress Cataloging-in-Publication Data, Philadelphia, PA, USA.
39. Zhou S, Sun B, Shi J (2006) An SPC monitoring system for cycle-based waveform signals using Haar transform. Autom Sci Eng IEEE Trans 3: 60-72.
40. Kosanovich KA, Piovoso MJ (1997) PCA of wavelet transformed process data for monitoring. Intell Data Anal 1: 85-99.
41. Nounou MN, Nounou HN, Meskin N (2012) Multiscale denoising of biological data: a comparative analysis. IEEE/ACM Trans Comput Biol Bioinform 9: 1539-1544.
42. Nounou MN, Bakshi BR (2000) Multiscale methods for denoising and compression. In: Walczak B (ed), Wavelets Chem. Elsevier Science BV, pp: 119-150.
43. Box GEP, Jenkins GM, Reinsel GC (2008) Time Series Analysis: Forecasting and Control. 4th edn. John Wiley & Sons, Inc., Hoboken, NJ, USA.

44. Thode HCJ (2002) Testing for Normality. 1st edn. CRC Press, New York, NY, USA.

45. Sheriff MZ, Harrou F, Nounou M (2014) Univariate process monitoring using multiscale Shewhart charts. (2014) Int Conf Control Decis Inf Technol (IEEE), pp: 435-440.

46. Sheriff MZ, Nounou MN (2016) Enhanced performance of shewhart charts using multiscale representation. In: 2016 Am. Control Conf. IEEE, Boston, MA, USA, pp: 6923-6928.

47. Sheriff MZ, Nounou M (2016) Fault detection using multiscale Shewhart charts: Algorithms and applications. 2016 AIChE Spring Meet. Fuels Petrochemicals Div.

48. Aradhye H, Bakshi B, Strauss R, Davis J (2003) Multiscale SPC using wavelets: theoretical analysis and properties. AIChE J 49: 939-958.

49. Dekermenjian M, Reza A, Koonce M, Poblotzki J (2003) Exothermic reactions between cryogenic fluorine, nitrogen trifluoride and stainless steel. 37th Annu. Loss Prev. Symp. AIChE Spring Natl. Meet.

50. Madakyaru M, Nounou M, Nounou H (2012) Linear inferential modeling: theoretical perspectives, extensions, and comparative analysis. Intell Control Autom 3: 376-389.